Ethiopian Journal of Natural and computational Science(EJNCS)

Ethiop J Nat Comp Sci 2023, Volume 3, Issue 1

Original Research Article

Dynamical Analysis of Cholera Diseases Transmission Model with Hospitalization

Haileyesus Tessema [1*] Gossay Aliy [1] Litegebe Wondie [1] Samuel Abebe [1] Sisay Ayanaw [1] Yehualashet Mengistu [1] Daniel Makinde [2] Hailay Weldegiorgis[3]

[1]Department of Mathematics, University of Gondar, Gondar, Ethiopia

[2]Faculty of Military Science, Stellenbosch University, Stellenbosch, South Africa.

[3]Department of Mathematics, Mekelle University, Mekelle, Ethiopia

* Correspondence: haila.tessema@gmail.com

Article History:
Received: 03 December 2022
Accepted: 13 February 2023
Published: 19 February 2023

Print ISSN 2710-0200
Electronic ISSN 2710-0219

ABSTRACT

In this work, a deterministic mathematical model was constructed to describe the transmission dynamics of cholera through both direct and indirect contact routes. The model is composed of five compartments: susceptible individuals, infectious individuals, hospitalized individuals, recovered individuals, and the *Vibrio cholerae* bacteria present in the environment. The qualitative features of the model—including the invariant region, the existence of a positive invariant solution, and the two equilibrium states (disease-free and endemic)—were analyzed, together with their local and global stability properties. Furthermore, the basic reproduction number was determined. Sensitivity analysis and numerical simulations were also carried out, revealing that minimizing contact rates, increasing hospitalization, and enhancing environmental sanitation are the most effective strategies for controlling cholera transmission within the population.

Keywords: Cholera, *Vibro cholerae*, DFE & EE, Stability Analysis , Numerical Simulation.

1 Introduction

In many countries around the globe—particularly in resource-limited regions—cholera remains a serious and persistent public health concern [Usmani et al., 2021]. Among infectious diseases, cholera stands out as a highly contagious illness that is endemic across large parts of Africa and Asia. It is caused by infection of the intestine with the bacterium *Vibrio cholerae* [Abubakar and Ibrahim, 2022].

The disease is extremely virulent and can lead to death within a short period, posing a continual threat to public health in developing nations, where cyclical outbreaks often occur twice annually in endemic areas [Koelle, 2009]. Globally, it is estimated that 3–5 million cases and over 100,000 deaths occur each year. Recent outbreaks have been concentrated mainly in Africa, especially in sub-Saharan regions [Sun et al., 2017]. Since the beginning of 2023, more than fourteen African countries—including Nigeria, Cameroon, the Democratic Republic of Congo, South Sudan, Somalia, Ethiopia, Kenya, Tanzania, Zambia, Malawi, Mozambique, Zimbabwe, South Africa, Eswatini, and Burundi—have reported cases of cholera [Gashaw Adane Erkyihun and Woldegiorgis, 2023].

Cholera has affected human populations for centuries and is primarily transmitted through the consumption of water contaminated with *Vibrio cholerae*. The bacteria are typically found in food or water contaminated by the feces of infected individuals [Usmani et al., 2021]. Outbreaks are most common in areas with poor sanitation, insufficient water treatment, and inadequate hygiene practices [Gashaw Adane Erkyihun and Woldegiorgis, 2023]. Transmission occurs through both *direct* and *indirect* pathways [Wang, 2022]. Direct, human-to-human transmission happens through contact with an infected person (e.g., touching, biting, or sexual contact), while indirect, environment-to-human transmission occurs through the ingestion of contaminated food or water. The disease spreads rapidly in areas lacking proper sewage treatment and safe drinking water systems [Gashaw Adane Erkyihun and Woldegiorgis, 2023, Challa et al., 2022].

To better understand, predict, and control infectious diseases such as cholera, epidemiologists and researchers frequently employ *mathematical modeling and numerical simulation*. These tools enable scientific exploration of disease dynamics, sensitivity to parameters, and forecasting of potential outbreaks. Various mathematical models have been developed to study cholera transmission. Some researchers have applied *deterministic models* [Nyabadza et al., 2019, Mukandavire and Morris Jr, 2015, Buliva et al., 2023, Yang et al., 2019, Sulayman, 2014], while others have utilized *stochastic models* [Tilahun et al.,

2020, Iddrisu et al., 2023].

For instance, Shelton et al. [2019] proposed an SIR-B model to investigate cholera dynamics. Nyabadza et al. [2019] examined cholera transmission under limited healthcare resources and found that their model exhibited backward bifurcation and multiple equilibria, concluding that increasing hospital capacity significantly reduces infection levels. Similarly, Ezeagu et al. [2019] developed a model incorporating quarantine and vaccination as control strategies and demonstrated that effective quarantine, vaccination, and proper sanitation can substantially reduce cholera transmission. More recently, Onitilo et al. [2023] proposed an SIR-V model to study cholera spread. Other scholars have explored *fractional-order models* [Rosa and Torres, 2021, Baba et al., 2023] and *optimal control approaches* [Berhe, 2020, Bakare and Hoskova-Mayerova, 2021, Abubakar and Ibrahim, 2022].

However, none of these studies have examined the *combined effect of both direct and indirect transmission pathways together with hospitalization of infectious individuals*. This paper aims to address this gap by developing a deterministic mathematical model that incorporates these aspects into the cholera transmission dynamics.

The remainder of this study is organized as follows: Section 1 presents the background and a review of related literature. Section 2 provides the formulation and description of the proposed model. Section 3 contains the model analysis, while Section 4 discusses numerical simulations and model calibration. Finally, Section 5 offers concluding remarks and insights.

2 Model Description and Formulation

In this study, the total population, denoted by $N(t)$, is divided into four epidemiological compartments based on disease status at time t: $S(t)$ — susceptible individuals, $I(t)$ — infected individuals, $H(t)$ — hospitalized individuals, and $R(t)$ — recovered individuals. Additionally, $C(t)$ represents the concentration of *Vibrio cholerae* bacteria present in the environment at time t.

New susceptible individuals enter the population through birth or immigration at a constant recruitment rate Π. All individuals experience natural mortality at a rate μ, which accounts for both natural and population-dependent death rates. Susceptible individuals may acquire cholera infection through direct contact with infected individuals or through indirect contact with contaminated environmental reservoirs at a combined

force of infection given by

$$\lambda = \beta I + b\beta C,$$

where β is the effective contact rate and b measures the relative contribution of environmental transmission.

Thus, the susceptible population increases at rate Π, but decreases due to natural death (μ) and infection (λ). The infected population increases through new infections (λ) and decreases by natural death (μ), disease-induced death (τ), hospitalization at rate $(1-\alpha)\omega$, and recovery at rate $\alpha\omega$. A fraction $(1-\alpha)$ of infected individuals move to the hospitalized compartment, while the remaining fraction α recovers naturally.

The hospitalized compartment gains individuals from the infected class at rate $(1-\alpha)\omega$ and loses them through recovery at rate φ and natural death at rate μ. The recovered population increases due to recovery from both hospitalization (φ) and natural recovery from infection ($\alpha\omega$), but decreases by natural death (μ).

Furthermore, infected individuals shed *Vibrio cholerae* bacteria into the environment at a rate σ, thereby increasing the environmental concentration $C(t)$. The bacteria die or are removed from the environment at rate ϑ.

Table 1 presents the description of the parameters used in the model, and the corresponding flow diagram illustrating the transmission dynamics of cholera is depicted in Figure 1.

Based on the aforementioned assumptions, the transmission dynamics of the model are described by the following system of differential equations:

$$\begin{aligned}
\tfrac{dS}{dt} &= \Pi - (b\beta\, C + \beta\, I)\, S - \mu\, S, \\
\tfrac{dI}{dt} &= (b\beta\, C + \beta\, I)\, S - (\omega + \tau + \mu)\, I, \\
\tfrac{dH}{dt} &= (1-\alpha)\,\omega I - (\mu + \varphi)\, H, \\
\tfrac{dR}{dt} &= \alpha\,\omega I + \varphi H - \mu\, R, \\
\tfrac{dC}{dt} &= \sigma\, I - \vartheta C.
\end{aligned} \tag{2.1}$$

The model is analyzed under the following initial conditions:

$$S(0) = S_0 > 0, \quad I(0) = I_0 \geq 0, \quad H(0) = H_0 \geq 0, \quad R(0) = R_0 \geq 0, \quad C(0) = C_0 \geq 0. \tag{2.2}$$

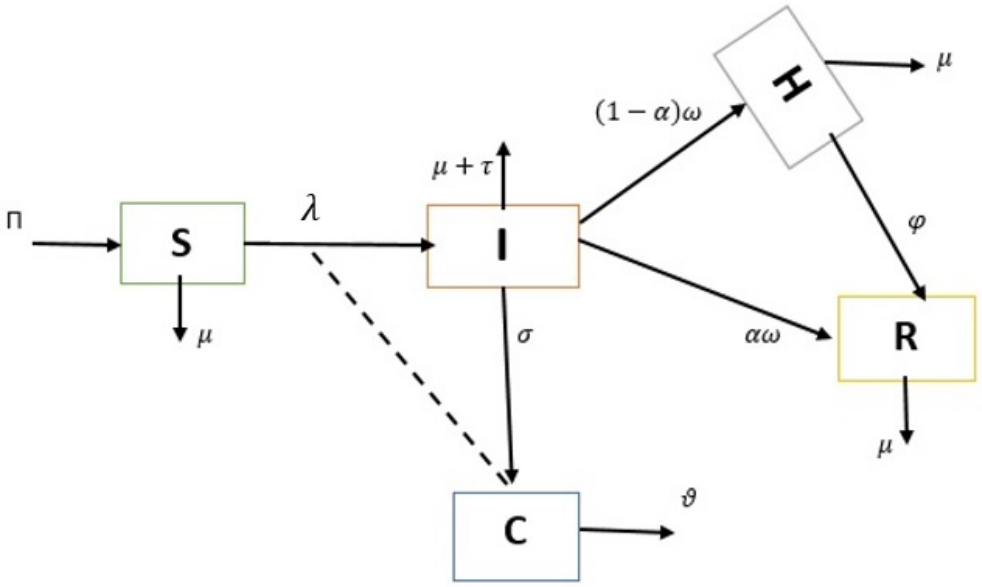

Figure 1: Flow diagram representing the transmission dynamics of cholera.

Table 1: Description of the parameters used in model (2.1).

Parameter	Description
Π	Recruitment rate of individuals into the population.
β	Effective contact rate of susceptible individuals.
τ	Disease-induced death rate among infected individuals.
ϑ	Natural clearance (decay) rate of *Vibrio cholerae* in the environment.
φ	Recovery rate of hospitalized individuals.
ω	Rate at which infected individuals leave the infectious compartment.
σ	Shedding rate of bacteria into the environment by infected individuals.
μ	Natural death rate of individuals.
α	Proportion of infected individuals who recover without hospitalization.

3 Model Analysis

3.1 Invariant Region

In this section, we identify a region in which the solutions of system (2.1) remain bounded and biologically meaningful. For the given model, the total human population at time t is defined as

$$N(t) = S(t) + I(t) + H(t) + R(t),$$

while $C(t)$ denotes the concentration of *Vibrio cholerae* in the environment.

Differentiating $N(t)$ with respect to time and substituting from system (2.1) gives:

$$\frac{dN}{dt} = \frac{dS}{dt} + \frac{dI}{dt} + \frac{dH}{dt} + \frac{dR}{dt} = \Pi - \tau I - \mu N.$$

In the absence of disease-induced mortality (i.e., $\tau = 0$), we have

$$\frac{dN}{dt} \leq \Pi - \mu N. \tag{3.1}$$

Solving Equation (3.1) and taking the limit as $t \to \infty$ yields

$$N(t) \longrightarrow \frac{\Pi}{\mu}.$$

Similarly, for the environmental bacterial concentration,

$$\frac{dC}{dt} = \sigma I - \vartheta C \leq \sigma \frac{\Pi}{\mu} - \vartheta C. \tag{3.2}$$

Solving Equation (3.2) and taking the limit as $t \to \infty$ gives

$$C(t) \longrightarrow \frac{\sigma \Pi}{\vartheta \mu}.$$

Hence, the feasible region for the system (2.1) is defined as

$$\Omega = \left\{ (S, I, H, R, C) \in \mathbb{R}_+^5 : 0 \leq S + I + H + R \leq \frac{\Pi}{\mu}, \quad 0 \leq C \leq \frac{\sigma \Pi}{\vartheta \mu} \right\}. \tag{3.3}$$

Therefore, Ω represents the biologically feasible and positively invariant region for the model (2.1), ensuring that all solutions of the system remain bounded within this region for all $t > 0$.

3.2 Positivity of Solutions

Theorem 3.1. *If $S(0) > 0$, $I(0) > 0$, $H(0) > 0$, $R(0) > 0$, and $C(0) > 0$ are positive initial conditions within the feasible region Ω, then the solution $(S(t), I(t), H(t), R(t), C(t))$ of system (2.1) remains positive for all $t \geq 0$.*

Proof. Let

$$\xi = \sup \{ t > 0 : S(\nu) \geq 0,\ I(\nu) \geq 0,\ H(\nu) \geq 0,\ R(\nu) \geq 0,\ C(\nu) \geq 0 \text{ for all } \nu \in [0, t] \}.$$

Since the initial conditions $S(0) > 0$, $I(0) > 0$, $H(0) > 0$, $R(0) > 0$, and $C(0) > 0$ hold, it follows that $\xi > 0$. If $\xi < \infty$, then at $t = \xi$, at least one of $S(\xi)$, $I(\xi)$, $H(\xi)$, $R(\xi)$, or $C(\xi)$ must become zero.

Consider the first equation of system (2.1):

$$\frac{dS}{dt} = \Pi - (b\beta\, C + \beta\, I + \mu)\, S. \tag{3.4}$$

Using the method of variation of constants, the solution of Equation (3.4) at $t = \xi$ can be written as

$$S(\xi) = S(0)\, \exp\left[-\int_0^{\xi} (b\beta\, C + \beta\, I + \mu)\, ds\right] + \int_0^{\xi} \Pi\, \exp\left[-\int_s^{\xi} (b\beta\, C + \beta\, I + \mu)\, d\nu\right] ds.$$

Because $\Pi > 0$ and all variables remain non-negative for $t \in [0, \xi]$, it follows that $S(\xi) > 0$. A similar argument can be applied to show that

$$I(\xi) > 0, \quad H(\xi) > 0, \quad R(\xi) > 0, \quad \text{and} \quad C(\xi) > 0.$$

This contradicts the assumption that any variable could become zero at $t = \xi$. Hence, $\xi = \infty$.

Therefore, all solution components of system (2.1) remain positive for all $t \geq 0$. □

3.3 Effective Reproduction Number and Disease-Free Equilibrium (DFE)

When the disease is absent from the population, that is, when $I = C = 0$, the system reaches a disease-free equilibrium (DFE). The DFE represents the steady state of the model in which no infection persists among the human population or in the environment. It is obtained by setting the right-hand sides of all equations in system (2.1) equal to zero and solving for the corresponding equilibrium values. Hence, the disease-free equilibrium point is given by:

3.4 Effective Reproduction Number and Disease-Free Equilibrium (DFE)

When the disease is absent from the population, i.e., $I = C = 0$, the system attains a disease-free equilibrium (DFE). By setting the right-hand sides of system (2.1) to zero, the DFE is obtained as:

$$E_0 = \left(\frac{\Pi}{\mu},\, 0,\, 0,\, 0,\, 0\right). \tag{3.5}$$

The effective reproduction number, denoted by $\mathcal{R}_0$, is computed using the next-generation

matrix approach as described in [Van den Driessche and Watmough, 2002]. To apply this method, the model equations are rewritten by focusing on the newly infected compartments as follows:

$$\begin{aligned} \frac{dI}{dt} &= (b\beta\, C + \beta\, I)\, S - (\omega + \tau + \mu)\, I, \\ \frac{dC}{dt} &= \sigma I - \vartheta C. \end{aligned} \tag{3.6}$$

At the DFE, the corresponding Jacobian matrices $\mathcal{F}$ and $\mathcal{V}$ are given by:

$$\mathcal{F} = \begin{pmatrix} \dfrac{\beta\,\Pi}{\mu} & \dfrac{b\beta\,\Pi}{\mu} \\ 0 & 0 \end{pmatrix}, \qquad \mathcal{V} = \begin{pmatrix} \omega + \tau + \mu & 0 \\ -\sigma & \vartheta \end{pmatrix}.$$

Hence, the next-generation matrix is computed as:

$$\mathcal{F}\mathcal{V}^{-1} = \begin{pmatrix} \dfrac{\beta\,\Pi}{\mu(\omega + \tau + \mu)} + \dfrac{\Pi\, b\beta\,\sigma}{\mu(\omega + \tau + \mu)\vartheta} & \dfrac{b\beta\,\Pi}{\mu\,\vartheta} \\ 0 & 0 \end{pmatrix}.$$

Therefore, the effective reproduction number is obtained as:

$$\mathcal{R}_{\text{Eff}} = \frac{\beta\,\Pi\ (b\sigma + \vartheta)}{\mu\,\vartheta\ (\omega + \tau + \mu)} = \mathcal{R}^{C}_{\text{Eff}} + \mathcal{R}^{I}_{\text{Eff}}, \tag{3.7}$$

where

$$\mathcal{R}^{I}_{\text{Eff}} = \frac{\beta\,\Pi\,\vartheta}{\mu\,\vartheta\,(\omega + \tau + \mu)} \quad \text{and} \quad \mathcal{R}^{C}_{\text{Eff}} = \frac{\beta\,\Pi\, b\sigma}{\mu\,(\omega + \tau + \mu)}.$$

The quantity $\mathcal{R}_{\text{Eff}}$ serves as a threshold parameter that represents the average number of new infections generated by a single infectious individual introduced into a wholly susceptible population [Van den Driessche and Watmough, 2002].

Theorem 3.2. *The disease-free equilibrium (DFE) point E_0 is locally asymptotically stable if $\mathcal{R}_{Eff} < 1$, and unstable if $\mathcal{R}_{Eff} > 1$.*

Proof. The Jacobian matrix of system (2.1) evaluated at the DFE E_0 is given by:

$$J = \begin{pmatrix} -\mu & -\frac{\beta\,\Pi}{\mu} & 0 & 0 & -\frac{b\beta\,\Pi}{\mu} \\ 0 & \frac{\beta\,\Pi}{\mu} - (\omega+\tau+\mu) & 0 & 0 & \frac{b\beta\,\Pi}{\mu} \\ 0 & (1-\alpha)\omega & -(\mu+\varphi) & 0 & 0 \\ 0 & \alpha\omega & \varphi & -\mu & 0 \\ 0 & \sigma & 0 & 0 & -\vartheta \end{pmatrix}.$$

The eigenvalues of this matrix include $-\mu$ and $-(\mu+\varphi)$, while the remaining two eigenvalues are determined from the characteristic equation:

$$\lambda^2 + \psi_1\lambda + \psi_2 = 0, \tag{3.8}$$

where

$$\psi_1 = \mu(\omega+\tau+\mu)\left[\frac{\vartheta}{\omega+\tau+\mu} + 1 - \mathcal{R}_{\text{Eff}}\right],$$

$$\psi_2 = \mu\,\vartheta\,(\omega+\tau+\mu)\,(1-\mathcal{R}_{\text{Eff}})\,.$$

According to the Routh–Hurwitz stability criterion, the roots of equation (3.8) have negative real parts if and only if

$$\psi_1 > 0, \quad \psi_2 > 0, \quad \text{and} \quad \psi_1\psi_2 > 0.$$

It is clear that both ψ_1 and ψ_2 are positive whenever $\mathcal{R}_{\text{Eff}} < 1$.

Therefore, all eigenvalues of the Jacobian have negative real parts when $\mathcal{R}_{\text{Eff}} < 1$, implying that the DFE is *locally asymptotically stable*. Conversely, when $\mathcal{R}_{\text{Eff}} > 1$, at least one eigenvalue becomes positive, making the DFE *unstable*. □

Theorem 3.3. *The disease-free equilibrium (DFE) point E_0 of the model (2.1) is globally asymptotically stable if $\mathcal{R}_{Eff} < 1$, and unstable if $\mathcal{R}_{Eff} > 1$.*

Proof. Consider the Lyapunov function

$$L = \psi_1 I + \psi_2 C. \tag{3.9}$$

Differentiating equation (3.9) with respect to t gives

$$\frac{dL}{dt} = \psi_1 \frac{dI}{dt} + \psi_2 \frac{dC}{dt}. \tag{3.10}$$

Substituting $\frac{dI}{dt}$ and $\frac{dC}{dt}$ from the model (2.1), we obtain

$$\begin{aligned}\frac{dL}{dt} &= \psi_1 \left[(b\beta C + \beta I)S - (\omega + \tau + \mu)I\right] + \psi_2[\sigma I - \vartheta C] \\ &= \vartheta \left[\psi_1 \frac{b\beta\Pi}{\vartheta\mu} - \psi_2\right] C + \left[(\omega + \tau + \mu)\left(\psi_1 \frac{\beta\Pi}{\mu(\omega + \tau + \mu)} - 1\right) + \psi_2\sigma\right] I.\end{aligned}$$

Now, let

$$\psi_1 = \frac{\sigma}{\omega + \tau + \mu}\psi_2.$$

Then, the derivative becomes

$$\frac{dL}{dt} = \vartheta\psi_2 \left[\frac{b\beta\Pi\sigma}{\vartheta\mu(\omega + \tau + \mu)} - 1\right] C + \psi_2\sigma \left[\frac{\beta\Pi}{\mu(\omega + \tau + \mu)} - 1 + 1\right] I.$$

Taking $\psi_2 = 1$ and substituting the expression for $\mathcal{R}_{\text{Eff}}$, we get

$$\frac{dL}{dt} = \vartheta \left(\mathcal{R}_{\text{Eff}}^C - 1\right) C + \sigma\mathcal{R}_{\text{Eff}}^I I.$$

For $S \leq S^0 = \dfrac{\Pi}{\mu}$, it follows that

$$\frac{dL}{dt} \leq 0 \quad \text{whenever} \quad \mathcal{R}_{\text{Eff}} < 1,$$

and equality holds, i.e. $\frac{dL}{dt} = 0$, if and only if $I = C = 0$.

Hence, the only invariant set where $\frac{dL}{dt} = 0$ is the DFE point E_0. By **LaSalle's Invariance Principle**, the equilibrium point E_0 is globally asymptotically stable in the feasible region Ω whenever $\mathcal{R}_{\text{Eff}} < 1$. □

3.5 The Endemic Equilibrium Point (EEP)

If $S(t) > 0$, $I(t) \geq 0$, $H(t) \geq 0$, $R(t) \geq 0$, and $C(t) \geq 0$, then there exists an equilibrium point called the *Endemic Equilibrium Point (EEP)*, denoted by

$$E^* = (S^*, I^*, H^*, R^*, C^*) \neq 0.$$

The endemic equilibrium occurs when the number of individuals in each compartment remains constant over time, that is,

$$\frac{dS}{dt} = \frac{dI}{dt} = \frac{dH}{dt} = \frac{dR}{dt} = \frac{dC}{dt} = 0.$$

Solving the system of equations obtained by setting the right-hand sides of model (2.1) to zero gives the following expressions for the equilibrium values:

$$\begin{aligned}
S^* &= \frac{\vartheta(\omega+\tau+\mu)}{\beta(b\sigma+\vartheta)},\\
I^* &= \frac{\vartheta\mu(\mathcal{R}_{\text{Eff}}-1)}{\beta(b\sigma+\vartheta)},\\
H^* &= \frac{(1-\alpha)\,\mu\vartheta(\mathcal{R}_{\text{Eff}}-1)}{(\mu+\varphi)(b\sigma+\vartheta)},\\
R^* &= \frac{(\alpha\mu+\varphi)\,\mu\vartheta(\mathcal{R}_{\text{Eff}}-1)}{(\mu+\varphi)(b\sigma+\vartheta)},\\
C^* &= \frac{\sigma\mu(\mathcal{R}_{\text{Eff}}-1)}{\beta(b\sigma+\vartheta)}.
\end{aligned}$$

Theorem 3.4. *The endemic equilibrium E^* of system (2.1) is locally asymptotically stable in the feasible region Ω if $\mathcal{R}_{Eff} > 1$.*

Proof. The Jacobian matrix of system (2.1) evaluated at the endemic equilibrium E^* is

$$J = \begin{pmatrix}
-b\beta C-\beta I-\mu & -\beta S & 0 & 0 & -b\beta S\\
b\beta C+\beta I & \beta S-\mu-\omega-\tau & 0 & 0 & b\beta S\\
0 & (1-\alpha)\omega & -\mu-\varphi & 0 & 0\\
0 & \alpha\omega & \varphi & -\mu & 0\\
0 & \sigma & 0 & 0 & -\vartheta
\end{pmatrix}. \tag{3.11}$$

From Equation (3.11), two eigenvalues can be immediately identified as

$$\lambda_1 = -\mu < 0 \quad \text{and} \quad \lambda_2 = -(\mu+\varphi) < 0.$$

The remaining eigenvalues are obtained from the characteristic polynomial

$$\lambda^3 + \varphi_1\lambda^2 + \varphi_2\lambda + \varphi_3 = 0, \tag{3.12}$$

where

$$\varphi_1 = \left[\frac{\sigma\mu(\omega+\tau+\mu)}{\vartheta(b\sigma+\vartheta)}\right](\beta(b\sigma+\vartheta)-1)+\beta(\vartheta+\mu)+\mu(\mathcal{R}_{\text{Eff}}-1),$$

$$\varphi_2 = \chi_1 - \chi_2,$$

$$\varphi_3 = \mu\vartheta(\omega+\tau+\mu)\mathcal{R}_{\text{Eff}} > 0,$$

with

$$\chi_1 = \big((\omega+\tau)(\sigma+\vartheta)+\vartheta(\vartheta+\mu)\big)\frac{\mu(\mathcal{R}_{\text{Eff}}-1)}{b\sigma+\vartheta}+\mu(\omega+\tau+\mu)(\vartheta+\mu)+\vartheta\mu,$$

$$\chi_2 = \frac{b\sigma\mu(\vartheta+\mu)(\mathcal{R}_{\text{Eff}}-1)}{b\sigma+\vartheta}+\frac{\sigma\mu(\omega+\tau+\mu)}{b\sigma+\vartheta}+\vartheta(\omega+\tau+\mu).$$

According to the **Routh–Hurwitz criterion**, all roots of the characteristic polynomial have negative real parts if and only if

$$\varphi_1 > 0, \quad \varphi_2 > 0, \quad \varphi_3 > 0, \quad \text{and} \quad \varphi_1\varphi_2 - \varphi_3 > 0.$$

These conditions hold whenever $\mathcal{R}_{\text{Eff}} > 1$. Therefore, the endemic equilibrium E^* is *locally asymptotically stable*. □

3.6 Bifurcation Analysis

Bifurcation refers to a qualitative change in the behavior of the solution trajectories of a dynamical system due to variations in a parameter. The specific parameter value at which this qualitative change occurs is called the *bifurcation point*. At this point, the number of equilibrium points, their stability properties, or both may change.

In the context of infectious disease modeling, the system may exhibit different dynamics depending on the effective reproduction number, $\mathcal{R}_{\text{Eff}}$. To examine the nature of the bifurcation in our cholera model, we apply the method based on **center manifold theory**, as introduced by Castillo-Chavez and Song [2004].

Theorem 3.5 (Castillo-Chavez and Song [2004])**.** *Consider a general system of ODEs with a parameter ϕ:*

$$\frac{dx}{dt} = f(x,\phi), \quad f:\mathbb{R}^n\times\mathbb{R}\longrightarrow\mathbb{R}^n, \quad f\in C^2(\mathbb{R}^n\times\mathbb{R}), \tag{3.13}$$

where $x=0$ is an equilibrium point, i.e., $f(0,\phi)\equiv 0$ for all ϕ. Assume the following conditions

hold:

M₁: $A = D_x f(0,0) = \left(\frac{\partial f_i}{\partial x_j}(0,0)\right)$ *is the linearization matrix of the system at* $x = 0$ *with* $\phi = 0$. *Zero is a simple eigenvalue of* A, *and all other eigenvalues have negative real parts.*

M₂: A *has a nonnegative right eigenvector* w *and a left eigenvector* v *corresponding to the zero eigenvalue.*

Let f_k *denote the* k*-th component of* f, *and define*

$$a = \sum_{k,i,j=1}^{n} v_k w_i w_j \frac{\partial^2 f_k}{\partial x_i \partial x_j}(0,0), \quad b = \sum_{k,i=1}^{n} v_k w_i \frac{\partial^2 f_k}{\partial x_i \partial \phi}(0,0).$$

Then, the local dynamics of (3.13) near $x = 0$ *are determined by* a *and* b *as follows:*

1. $a > 0, b > 0$*: For* $\phi < 0$ *with* $|\phi| \ll 1$, $x = 0$ *is locally asymptotically stable and a positive unstable equilibrium exists; for* $0 < \phi \ll 1$, $x = 0$ *is unstable and a negative locally asymptotically stable equilibrium exists.*

2. $a < 0, b < 0$*: For* $\phi < 0$ *with* $|\phi| \ll 1$, $x = 0$ *is unstable; for* $0 < \phi \ll 1$, $x = 0$ *is locally asymptotically stable and a positive unstable equilibrium exists.*

3. $a > 0, b < 0$*: For* $\phi < 0$ *with* $|\phi| \ll 1$, $x = 0$ *is unstable and a locally asymptotically stable negative equilibrium exists; for* $0 < \phi \ll 1$, $x = 0$ *is stable and a positive unstable equilibrium appears.*

4. $a < 0, b > 0$*: As* ϕ *changes from negative to positive,* $x = 0$ *changes from stable to unstable, and a negative unstable equilibrium becomes positive and locally asymptotically stable.*

In particular, if $a < 0$ *and* $b > 0$, *the bifurcation is forward; if* $a > 0$ *and* $b > 0$, *the bifurcation is backward. This approach can be applied to analyze the bifurcation behavior of the cholera model.*

Theorem 3.6. *The model in system (2.1) exhibits a forward bifurcation at* $\mathcal{R}_{Eff} = 1$.

Proof. We prove this using the center manifold theorem [Castillo-Chavez and Song, 2004].

Let

$$S = x_1, \quad I = x_2, \quad H = x_3, \quad R = x_4, \quad C = x_5,$$

and define the vector $x = (x_1, x_2, x_3, x_4, x_5)^T$ with $\frac{dx}{dt} = F(x)$, $F = (f_1, f_2, f_3, f_4, f_5)^T$. Then system (2.1) can be rewritten as

$$\begin{aligned}
\frac{dx_1}{dt} &= \Pi - (b\beta x_5 + \beta x_2)x_1 - \mu x_1,\\
\frac{dx_2}{dt} &= (b\beta x_5 + \beta x_2)x_1 - (\omega + \tau + \mu)x_2,\\
\frac{dx_3}{dt} &= (1-\alpha)\omega x_2 - (\mu + \varphi)x_3,\\
\frac{dx_4}{dt} &= \alpha\omega x_2 + \varphi x_3 - \mu x_4,\\
\frac{dx_5}{dt} &= \sigma x_2 - \vartheta x_5.
\end{aligned} \tag{3.14}$$

We consider the disease transmission rate β as the bifurcation parameter, so that $\mathcal{R}_{Eff} = 1$ iff

$$\beta = \beta^* = \frac{\mu\vartheta(\omega + \tau + \mu)}{\Pi(b\sigma + \vartheta)}.$$

The disease-free equilibrium (DFE) is

$$E_0 = \left(\frac{\Pi}{\mu}, 0, 0, 0, 0\right).$$

The Jacobian matrix of (3.14) at the DFE is

$$J = \begin{pmatrix}
-\mu & -\frac{\beta\Pi}{\mu} & 0 & 0 & -\frac{b\beta\Pi}{\mu}\\
0 & \frac{\beta\Pi}{\mu} - (\omega + \tau + \mu) & 0 & 0 & \frac{b\beta\Pi}{\mu}\\
0 & (1-\alpha)\omega & -\mu - \varphi & 0 & 0\\
0 & \alpha\omega & \varphi & -\mu & 0\\
0 & \sigma & 0 & 0 & -\vartheta
\end{pmatrix}.$$

Zero is a simple eigenvalue of J at $\beta = \beta^*$. The corresponding right eigenvector $w = (w_1, w_2, w_3, w_4, w_5)^T$ satisfies $Jw = 0$, giving

$$\begin{aligned}
w_1 &= -\frac{\omega + \tau + \mu}{\mu\Pi}w_2, \quad w_2 = w_2 > 0,\\
w_3 &= \frac{(1-\alpha)\omega}{\varphi + \mu}w_2, \qquad w_4 = \frac{\omega(1-\alpha) + \omega(\varphi + \mu)}{\mu(\varphi + \mu)}w_2,\\
w_5 &= \frac{\sigma}{\vartheta}w_2.
\end{aligned}$$

The left eigenvector $v = (v_1, v_2, v_3, v_4, v_5)$ satisfies $v^T J = 0$, giving

$$v_1 = v_3 = v_4 = 0, \quad v_5 = \frac{b(\omega + \tau + \mu)}{b\sigma + \vartheta} v_2,$$

with v_2 chosen such that $v \cdot w = 1$.

Using the nonzero second derivatives of f_2:

$$\frac{\partial^2 f_2}{\partial x_1 \partial x_5} = \frac{\partial^2 f_2}{\partial x_5 \partial x_1} = \beta^*, \quad \frac{\partial^2 f_2}{\partial x_2 \partial x_5} = \frac{\partial^2 f_2}{\partial x_5 \partial x_2} = b\beta^*,$$

and

$$\frac{\partial^2 f_2}{\partial x_2 \partial \beta^*} = \beta^*, \quad \frac{\partial^2 f_2}{\partial x_5 \partial \beta^*} = b\beta^*,$$

we compute the bifurcation coefficients

$$a = -2\frac{\beta(\omega + \tau + \mu)}{\mu \Pi}\left(1 + \frac{b\sigma}{\vartheta}\right) < 0, \quad b = \beta\left(1 + \frac{b\sigma}{\vartheta}\right) > 0.$$

Since $a < 0$ and $b > 0$, the system exhibits a *forward bifurcation* at $\mathcal{R}_{Eff} = 1$. Therefore, there exists at least one stable endemic equilibrium when $\mathcal{R}_{Eff} > 1$.

Using I^* from the endemic equilibrium, a forward bifurcation diagram is plotted in Figure 2.

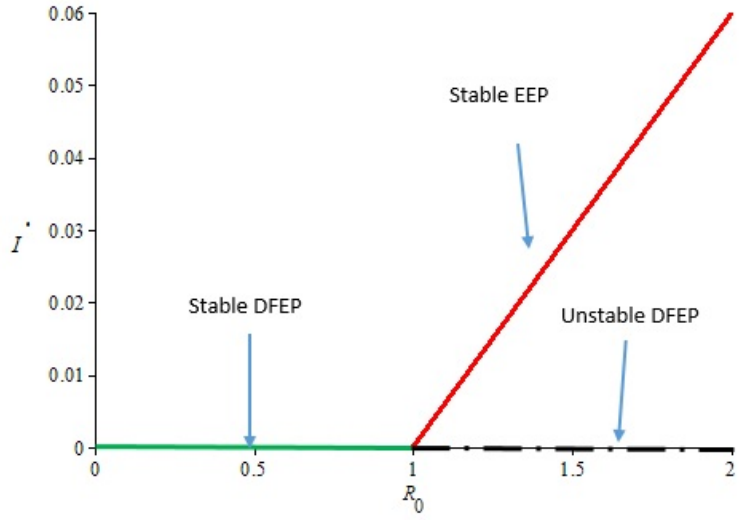

Figure 2: Forward bifurcation diagram of the cholera model.

□

3.7 Sensitivity Analysis

In this section, we perform sensitivity analysis to identify the parameters that have the most impact on the transmission of cholera. We use the normalized forward sensitivity index as defined in [Blower and Dowlatabadi, 1994] and applied in [Alemneh et al., 2023].

The normalized forward sensitivity index of a variable, $\mathcal{R}_{Eff}$, with respect to a parameter p, is defined as

$$\Lambda_p^{\mathcal{R}_{Eff}} = \frac{\partial \mathcal{R}_{Eff}}{\partial p} \cdot \frac{p}{\mathcal{R}_{Eff}},$$

where p represents any basic parameter of the model.

For our model,

$$\mathcal{R}_{Eff} = \frac{\beta \Pi (b\sigma + \vartheta)}{\mu\vartheta(\omega + \tau + \mu)}.$$

The sensitivity indices of $\mathcal{R}_{Eff}$ with respect to the parameters are:

$$\begin{aligned}
\Lambda_\beta^{\mathcal{R}_{Eff}} &= \frac{\partial \mathcal{R}_{Eff}}{\partial \beta} \cdot \frac{\beta}{\mathcal{R}_{Eff}} = 1 > 0, \\
\Lambda_b^{\mathcal{R}_{Eff}} &= \frac{\partial \mathcal{R}_{Eff}}{\partial b} \cdot \frac{b}{\mathcal{R}_{Eff}} = \frac{b\sigma}{b\sigma + \vartheta} > 0, \\
\Lambda_\mu^{\mathcal{R}_{Eff}} &= \frac{\partial \mathcal{R}_{Eff}}{\partial \mu} \cdot \frac{\mu}{\mathcal{R}_{Eff}} = -\frac{\mu}{\omega + \tau + \mu} < 0, \\
\Lambda_\tau^{\mathcal{R}_{Eff}} &= \frac{\partial \mathcal{R}_{Eff}}{\partial \tau} \cdot \frac{\tau}{\mathcal{R}_{Eff}} = -\frac{\tau}{\omega + \tau + \mu} < 0, \\
\Lambda_\omega^{\mathcal{R}_{Eff}} &= \frac{\partial \mathcal{R}_{Eff}}{\partial \omega} \cdot \frac{\omega}{\mathcal{R}_{Eff}} = -\frac{\omega}{\omega + \tau + \mu} < 0, \\
\Lambda_\sigma^{\mathcal{R}_{Eff}} &= \frac{\partial \mathcal{R}_{Eff}}{\partial \sigma} \cdot \frac{\sigma}{\mathcal{R}_{Eff}} = \frac{b\sigma}{b\sigma + \vartheta} > 0, \\
\Lambda_\vartheta^{\mathcal{R}_{Eff}} &= \frac{\partial \mathcal{R}_{Eff}}{\partial \vartheta} \cdot \frac{\vartheta}{\mathcal{R}_{Eff}} = -\frac{b\sigma}{b\sigma + \vartheta} < 0.
\end{aligned}$$

From the signs of these sensitivity indices, we see that β, b, and σ have a positive effect on $\mathcal{R}_{Eff}$, meaning that increases in these parameters increase disease transmission, whereas μ, τ, ω, and ϑ have a negative effect, decreasing $\mathcal{R}_{Eff}$ when increased.

Figure 3 illustrates the sensitivity indices of the effective reproduction number, $\mathcal{R}_{Eff}$, with respect to the basic parameters of the model. Parameters with positive sensitivity indices, such as Π, β, and σ, have a strong impact on the spread of cholera: increasing these parameters, while keeping others constant, tends to increase the disease burden in the community.

Conversely, parameters with negative sensitivity indices, including τ, ω, ϑ, and μ, act

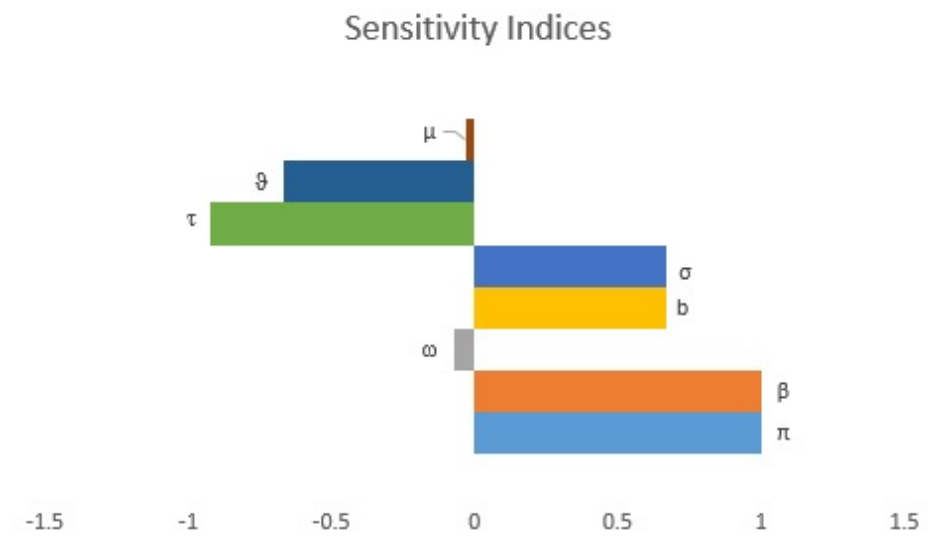

Figure 3: The local elasticity indices of $\mathcal{R}_{Eff}$ with respect to the parameters of model (1).

to reduce cholera transmission: increasing these parameters decreases the reproduction number and helps control the disease.

Based on these results, policymakers and public health stakeholders should focus on reducing the values of parameters with positive indices, for example: - lowering the transmission rate from infected humans (β), and - decreasing the shedding of Vibrio cholerae into the environment (σ),

while simultaneously increasing parameters with negative indices, such as: - enhancing the recovery rate of infected individuals (ω), and - improving the environmental clearance rate of Vibrio cholerae (ϑ).

Implementing these measures can effectively reduce $\mathcal{R}_{Eff}$ and help control cholera in the community.

4 Numerical Simulations

We perform numerical simulations of system (2.1) to support our theoretical findings. The simulations were implemented using Maple software and solved with the ODE45 solver. Using the parameter values listed in Table 2, we consider the initial conditions: $S(0) = 1000$, $I(0) = 100$, $R(0) = 0$, $H(0) = 10$, and $C(0) = 100$.

We first investigated the effect of varying the contact rate β between susceptible individuals and the *Vibrio cholerae* pathogen and infected individuals. Figure 4 (a)-(e) shows that as β increases from 0.002 to 0.006, the susceptible population (Figure 4a) decreases, while the infected (Figure 4b), hospitalized (Figure 4c), recovered (Figure 4d), and pathogen

Table 2: Parameter values for the Cholera model in (2.1)

Parameter symbol	Value	Source
Π	3.5	Assumed
β	0.002	[Berhe, 2020]
b	2	Assumed
σ	20	Assumed
ω	0.062	Assumed
α	0.44	[Berhe, 2020]
μ	0.0014	[Alemneh et al., 2023]
ϑ	0.033	[Berhe, 2020]
τ	0.015	[Tilahun et al., 2020, Berhe, 2020]
φ	0.2	[Tilahun et al., 2020]

populations (Figure 4e) increase over time. This indicates that reducing contact with infectious individuals and the pathogen can significantly lower the number of infected individuals in the population.

Next, we examined the effect of increasing the rate at which infected individuals leave the infected compartment, ω. Figure 5 (a)-(e) shows that as ω increases from 0.032 to 0.082, the susceptible population (Figure 5a), hospitalized (Figure 5c), and recovered (Figure 5d) populations increase, while the infected (Figure 5b) and pathogen populations (Figure 5e) decrease. Hence, increasing ω—for instance, through improved treatment or isolation—helps control the disease.

Finally, we explored the effect of varying the shedding rate of infectious individuals into the environment, σ. Figure 6 (a)-(e) illustrates that as σ increases from 0.2 to 0.5, the environmental pathogen population (Figure 6e) increases, leading to higher numbers of infected (Figure 6b), hospitalized (Figure 6c), and recovered (Figure 6d) individuals, while the susceptible population decreases (Figure 6a). This shows that reducing the shedding rate of infected individuals is critical to lowering the disease burden in the community.

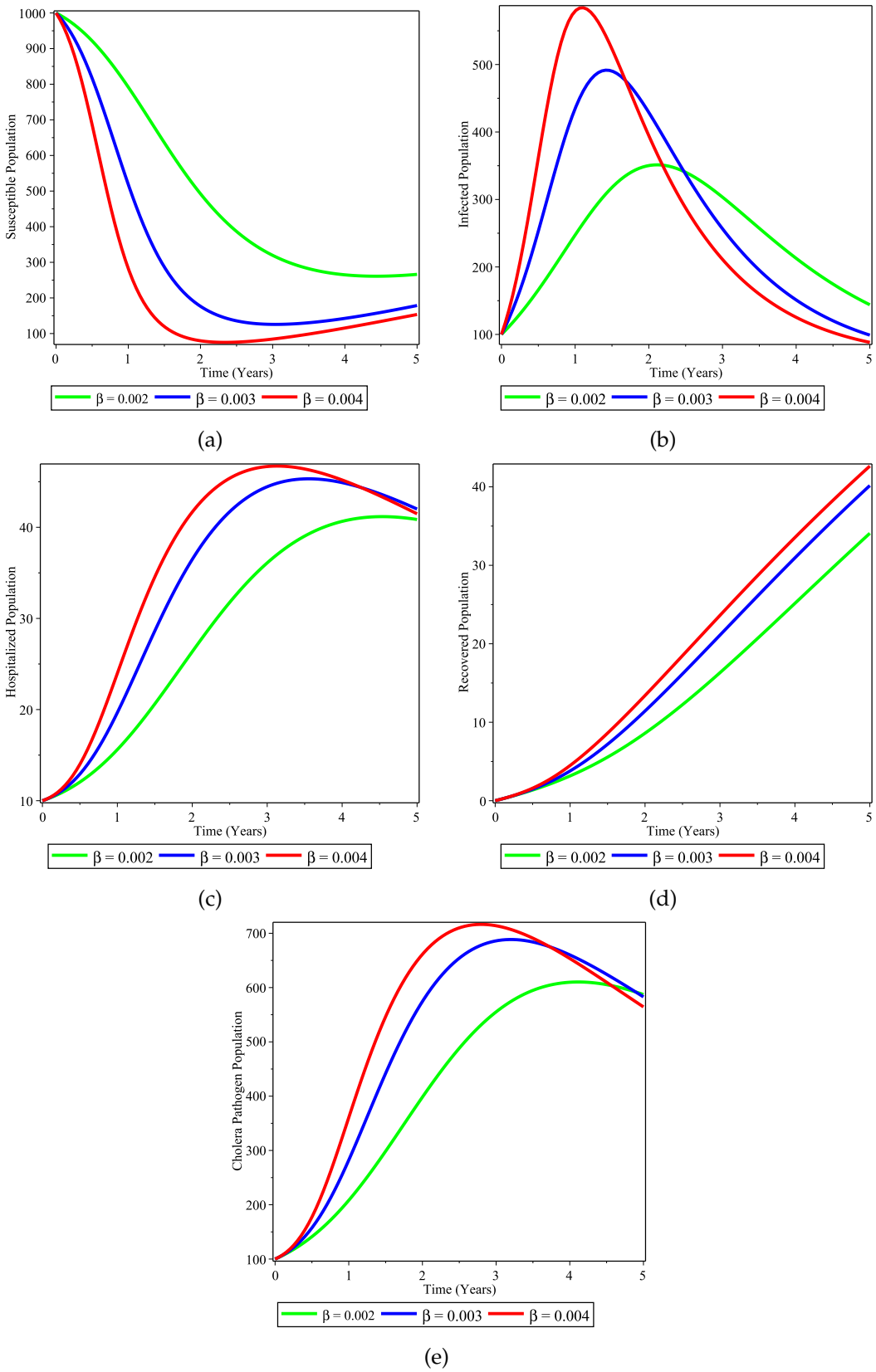

Figure 4: Simulations of the Cholera model for different value of β.

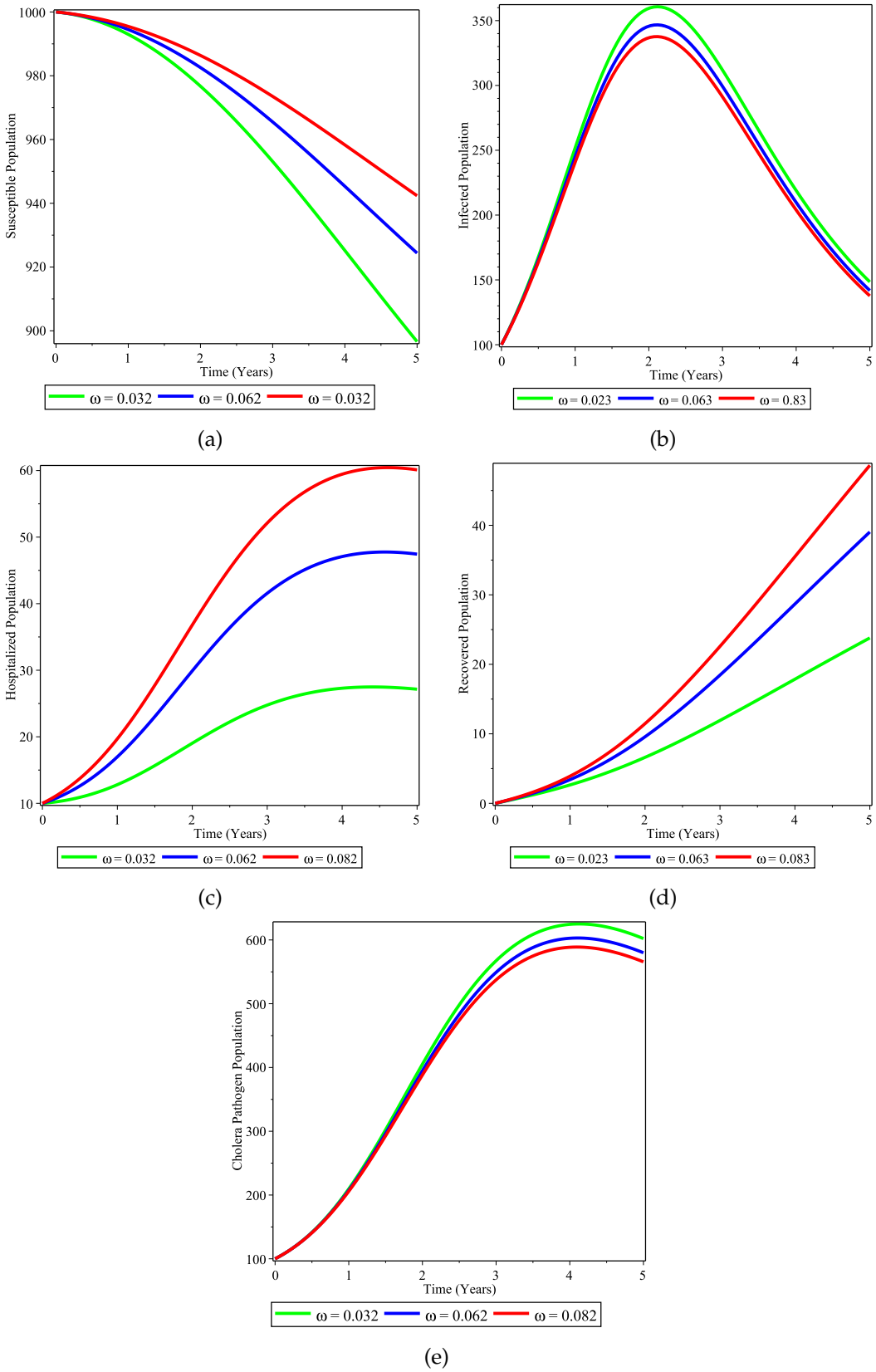

Figure 5: Simulations of the Cholera model for different value of ω.

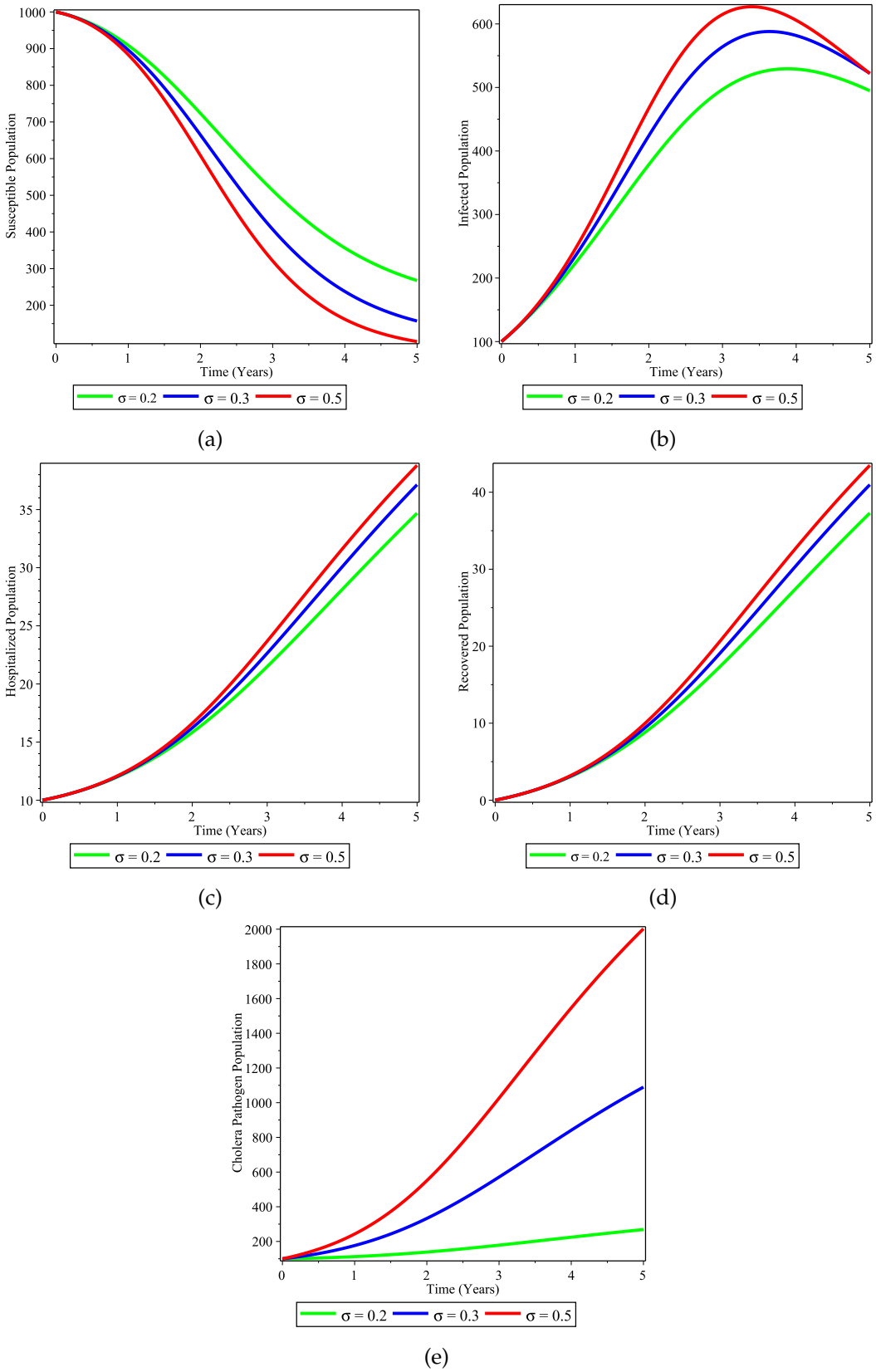

Figure 6: Simulations of the Cholera model for different value of σ.

5 Discussions and Conclusions

In this study, we developed an SIHR-C deterministic model to analyze the dynamics of cholera transmission. We investigated the qualitative behavior of the model and derived the effective reproduction number, which was used to examine the stability of the disease-free and endemic equilibrium points. The global stability of the disease-free equilibrium (DFE) was established using a Lyapunov function. Our bifurcation analysis revealed that the model exhibits a forward bifurcation, which differs from the findings of Sun et al. [2017], likely due to the assumption of mass-action incidence in our model.

A sensitivity analysis highlighted the influence of model parameters on cholera transmission. Parameters with positive sensitivity indices, such as β, σ, and Π, should be reduced, while parameters with negative indices, including ω, τ, and ϑ, should be increased to effectively control the disease. These results align with the recommendations of Berhe [2020].

From the simulations and analysis, it is evident that minimizing both direct and indirect contact rates significantly reduces the number of infected individuals, consistent with findings by Tilahun et al. [2020]. Additionally, enhancing treatment of infected individuals lowers infection prevalence and reduces the environmental concentration of *Vibrio cholerae*, as noted in Tilahun et al. [2020], Berhe [2020]. Therefore, policymakers and public health stakeholders play a crucial role in controlling cholera outbreaks in a short period of time.

Data Availability

The data used in this research are obtained from the cited published articles.

Conflict of Interest

The authors declare that there is no conflict of interest regarding this work.

Acknowledgments

The authors would like to express their sincere gratitude to the anonymous reviewers for their constructive comments and valuable suggestions, which greatly improved the

quality of this work.

References

S. F. Abubakar and M. Ibrahim. Optimal control analysis of treatment strategies of the dynamics of cholera. *Journal of Optimization*, 2022, 2022.

H. T. Alemneh, A. M. Belay, et al. Modelling, analysis, and simulation of measles disease transmission dynamics. *Discrete Dynamics in Nature and Society*, 2023, 2023.

I. A. Baba, U. W. Humphries, and F. A. Rihan. A well-posed fractional order cholera model with saturated incidence rate. *Entropy*, 25(2):360, 2023.

E. A. Bakare and S. Hoskova-Mayerova. Optimal control analysis of cholera dynamics in the presence of asymptotic transmission. *Axioms*, 10(2):60, 2021.

H. W. Berhe. Optimal control strategies and cost-effectiveness analysis applied to real data of cholera outbreak in ethiopia's oromia region. *Chaos, Solitons & Fractals*, 138: 109933, 2020.

S. M. Blower and H. Dowlatabadi. Sensitivity and uncertainty analysis of complex models of disease transmission: an hiv model, as an example. *International Statistical Review/Revue Internationale de Statistique*, pages 229–243, 1994.

E. Buliva, S. Elnossery, P. Okwarah, M. Tayyab, R. Brennan, and A. Abubakar. Cholera prevention, control strategies, challenges and world health organization initiatives in the eastern mediterranean region: A narrative review. *Heliyon*, 2023.

C. Castillo-Chavez and B. Song. Dynamical models of tuberculosis and their applications. *Mathematical biosciences and engineering*, 1(2):361–404, 2004.

J. M. Challa, T. Getachew, A. Debella, M. Merid, G. Atnafe, A. Eyeberu, A. Birhanu, and L. D. Regassa. Inadequate hand washing, lack of clean drinking water and latrines as major determinants of cholera outbreak in somali region, ethiopia in 2019. *Frontiers in public health*, 10:845057, 2022.

N. J. Ezeagu, H. A. Togbenon, and E. Moyo. Modeling and analysis of cholera dynamics with vaccination. *American Journal of Applied Mathematics and Statistics*, 7(1):1–8, 2019.

N. A. Gashaw Adane Erkyihun and A. Z. Woldegiorgis. The threat of cholera in africa. *Erkyihun et al. Zoonoses*, 42(3):1–6, 2023.

W. A. Iddrisu, I. Iddrisu, A.-K. Iddrisu, et al. Modeling cholera epidemiology using stochastic differential equations. *Journal of Applied Mathematics*, 2023, 2023.

K. Koelle. The impact of climate on the disease dynamics of cholera. *Clinical Microbiology and Infection*, 15:29–31, 2009.

Z. Mukandavire and J. G. Morris Jr. Modeling the epidemiology of cholera to prevent disease transmission in developing countries. *Microbiology spectrum*, 3(3):10–1128, 2015.

F. Nyabadza, J. M. Aduamah, and J. Mushanyu. Modelling cholera transmission dynamics in the presence of limited resources. *BMC Research Notes*, 12:1–8, 2019.

S. Onitilo, M. USMAN, D. DANIEL, T. ODULE, and A. SANUSİ. Modelling the transmission dynamics of cholera disease with the impact of control strategies in nigeria. *Cankaya University Journal of Science and Engineering*, 20(1):35–52, 2023.

S. Rosa and D. F. Torres. Fractional-order modelling and optimal control of cholera transmission. *Fractal and Fractional*, 5(4):261, 2021.

T. Shelton, E. Groves, and S. Adrian. A model of the transmission of cholera in a population with contaminated water. *CODEE Journal*, 12(1), 2019.

F. Sulayman. Modelling and analysis of the spread of cholera disease in nigeria with environmental control. *Research thesis*, 2014.

G.-Q. Sun, J.-H. Xie, S.-H. Huang, Z. Jin, M.-T. Li, and L. Liu. Transmission dynamics of cholera: Mathematical modeling and control strategies. *Communications in Nonlinear Science and Numerical Simulation*, 45:235–244, 2017.

G. T. Tilahun, W. A. Woldegerima, and A. Wondifraw. Stochastic and deterministic mathematical model of cholera disease dynamics with direct transmission. *Advances in Difference Equations*, 2020(1):1–23, 2020.

M. Usmani, K. D. Brumfield, Y. Jamal, A. Huq, R. R. Colwell, and A. Jutla. A review of the environmental trigger and transmission components for prediction of cholera. *Tropical Medicine and Infectious Disease*, 6(3):147, 2021.

P. Van den Driessche and J. Watmough. Reproduction numbers and sub-threshold endemic equilibria for compartmental models of disease transmission. *Mathematical biosciences*, 180(1):29–48, 2002.

J. Wang. Mathematical models for cholera dynamics—a review. *Microorganisms*, 10(12): 2358, 2022.

J. Yang, C. Modnak, and J. Wang. Dynamical analysis and optimal control simulation for an age-structured cholera transmission model. *Journal of the Franklin Institute*, 356(15): 8438–8467, 2019.